STUDY OF REDUNDANT CONSTRAINED DYNAMICS ANALYSIS METHOD FOR SUSPENSION AMUSEMENT EQUIPMENT

Guofa XU[1], Ping ZHAO[1,*], Yongkui LI[1], Zengxi LI[1]

In the analysis of rigid-body dynamics, the mating between parts has a significant impact on the simulation, making it difficult to obtain accurate results if redundant constraints exist. Using SolidWorks Motion, we modelled a large amusement equipment (Giant Frisbee) spindle to study the full load and dynamic characteristics of the spindle under redundant constraints and set the bushing parameters for the simulation between the spindle and both sides of the swing arm link. We then extracted the stress-time curves for each side of the link and compared with theoretical calculation. The results showed that the dynamics results obtained using the bushing tool are more consistent with the theoretical results. Therefore, the influence of redundant constraints must be considered in virtual prototyping to ensure the accuracy and reliability of the simulation results, and in turn, to correctly guide the structural design process. This study provides a valuable reference for the analysis of the dynamic characteristics of components under complex constraints.

Keywords: redundant constraints; amusement facilities; virtual prototype; rigid-body dynamics

1. Introduction

Currently, virtual prototype technology plays an important role in dynamic analysis of mechanical systems as it greatly simplifies the design and development process and improves design quality [1-3]. In practical application, it has been shown that when there are redundant constraints between the analyzed parts, virtual prototyping will produce inaccurate force estimates for the connected parts [4-5]. This problem is particularly prominent in the analysis of large equipment with complex motion and working conditions. At present, there are relatively few studies addressing this challenge, and those that exist are neither systematic nor universal [6-9]. Most of these studies also adopt a simplified model for analysis, which leads to a decrease in accuracy and restricts the application and promotion of virtual prototype technology. For example, amusement equipment of the large and gyroscopic type – such as the Giant Frisbee – is often simplified to a pendulum model, ignoring the influence of the gyroscopic effect. At the same time, the virtual prototype analysis does not fully consider the

[1] Engineering College, Shenyang Agricultural University, Shenyang 110866, China
*Corresponding author: Ping Zhao, e-mail: zhaopingxdg@163.com

influence of the redundant constraints problem, leading to errors in the dynamic characteristics of key node locations [10-12]. By comparing several simulations, it has been found that the redundant constraints problem has a significant influence on simulation results, and certain methods must be adopted accordingly to rectify these issues.

Based on the illustration above, this paper carries out the research on the redundant constraint problem of rigid-body dynamics. In this study, SolidWorks software and the Motion plug-in were used in combination to investigate the characteristics of the Giant Frisbee spindle under load conditions in simulation analysis. Furthermore, we explored how the software bushing tools treated the redundant constraints condition. Finally, we determined a method to obtain accurate simulation results, which can provide a reference for the dynamic characteristics of the parts with the complex constraint form.

2. Establishment of dynamic models

2.1 Basic design parameters

Due to the complex structure of amusement equipment, the complete equipment parameters cannot be obtained in the initial design stage. Therefore, it is necessary to simplify the structure based on assumptions prior to establishing the virtual prototype models. This simplification includes the variables related to dynamics such as the structure's main body size, mass, and the position of center of mass. If the resulting motion, component characteristics, damping and other parameter conditions are not significantly affected by the simplification and do not adversely affect the interaction between parts or the later strength analysis, the simplification and assumptions can be considered effective [13-14]. The basic design parameters of the Giant Frisbee according to the relevant design requirements and materials are shown in Table 1.

Table 1

Basic design parameters of Giant Frisbee

Size	Frisbee Diameter:10 m
	Swing Arm Length:15.5 m
Characteristics	Swing Arm Weight:8.5 tons
	Rotary Frisbee Weight:17.5 tons
	Movable Load:700 N/person
Other	Authorized Carrying Capacity:42 people
	Maximum Amplitude: ±120 degrees

The motion of the equipment is composed of the swinging of the swing arm and the rotation of frisbee, and its overall motion is like a gyroscope. Therefore, this equipment belongs to the category of large gyroscopic amusement equipment and the influence of the gyroscopic effect should be considered in analysis. The equipment is mainly composed of a rotary frisbee, a swing arm, a spindle, four frames and other parts shown in Figure 1. In SolidWorks, the "Top to Down" modeling method was adopted to create the required parts individually, and the masses of the parts were set through the "Override Mass Properties" function of the software. The turntable as a whole was created as a rigid sub-assembly.

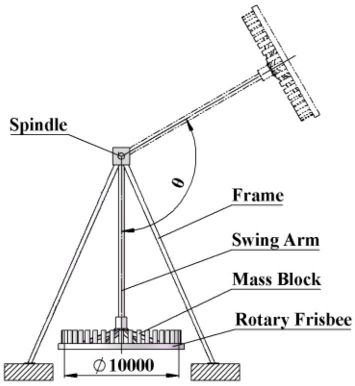

Fig. 1. Schematic diagram of the structure of the Giant Frisbee

2.2 Stress form analysis of spindle

Before starting assembly of the model, there was a need to analyze the stress of the main shaft form in order to judge which parts in the actual cases may be limited by the constraint reaction force. This information guides the addition of components in the constraint condition model, ensuring the analysis and simplification is rational. The constraint reaction force form of the spindle shown in Figure 2, and *L* represents the left and *R* represents the right.

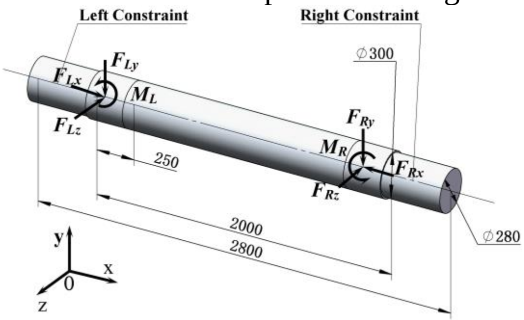

Fig. 2. Analysis diagram of constraint force form of spindle

From the figure:

F_{Lx}, F_{Rx}: The swing arm transfers the *x*-direction component of this spindle force through the bearing.

F_{Ly}, F_{Ry}: The swing arm transfers the *y*-direction component of this spindle force through the bearing.

F_{Lz}, F_{Rz}: The swing arm transfers the *z*-direction component of this spindle through the bearing.

M_L, M_R: The counter-torque transmitted by the swing arm to the spindle by the bearing.

The results showed that the spindle is consistently affected by axial force, radial force and reaction moment (perpendicular to the axis direction). In real-world cases, the swing arm and the spindle pass through the bearing connection. Thus, in the initial stage of designing the spindle, the SolidWorks "Hinge" function can be used instead of a bearing modelling a constraint. Furthermore, the constraints of the interaction between the frame and spindle do not need to be given when using the finite element method (FEM) for structural performance analysis as the constraints of the bearing clamp can be used directly.

2.3 Stress form analysis of spindle

According to the movement and connection of the mechanism, the model was assembled in the SolidWorks assembly environment. The relationship between the main parts is shown in Table 2, and geometric relations such as "Coincidence" and "Parallel" were added between the parts' datum planes to determine the initial position of the mechanism.

Table 2

Connection between parts

Object	Mate
Swing Arm-Spindle (Left)	"Hinge"
Swing Arm-Spindle (Right)	"Hinge"
Frame to Floor	"Fix"
Rotary Frisbee-Swing Arm	"Hinge"
Spindle-Frame	"Hinge"

2.4 Redundant constraints

In the rigid-body dynamics model, the geometric mate relationship is predominantly used, so the rigid mate relation is continued in the dynamic analysis. Rigid mating does not affect the solution of the kinematic mechanisms, but for the complex dynamic system, a rigid mate will repeatedly constrain the same degree of freedom (DOF) of the parts. This results in erroneous simulated force transfer routes and affects the accuracy of the final simulation results. In SolidWorks software, this situation is called "Redundancy".

2.4.1 The calculation of the redundant DOF

Redundant constraints are the inherent problems of rigid body dynamics simulation. This simply means that repeated constraints are added to a given degree of freedom in the matching mechanism [15]. If there is "redundancy" in the moving joint of interest, the software will determine this by calculating the

“Redundant DOF” as: Redundant DOF = Total Actual DOF - Total Estimated DOF.

When the "Redundant DOF" is negative, it indicates that there is a "Redundancy" problem. The magnitude of the value is indicative of the number of redundancies. In the assembled model, the spindle and the swing arm are joined by a “hinge” instead of the actual bearing links. As such, the swing arm has one “total actual DOF” around the axis of rotation while each of the two parts of the "hinge" have constraints of 5 degrees of freedom. Accordingly, "Total Estimated DOF" = 6-(2×5) = -4, and "Redundant DOF" = 1-(-4) = 5. This indicates that a "hinge" will cause redundant constraints on five degrees of freedom in the same direction.

2.4.2 Link parameter setting

The constraint reaction force transferred from the swing arm to the spindle can only be shared by the unilateral "hinge" as it is affected by the redundant constraints such that another "hinge " does not also transfer force. However, this does not conform to the real-world stress of the parts. There are three main ways to deal with "Redundancy" in SolidWorks software:

(1) Create a rigid group. In this method, the parts other than those being studied are created as a single rigid group, to be regarded as a single part, according to their independent motion form. In the simulation analysis, the software will automatically ignore the internal redundant constraints.

(2) Replace a complex mate with a simple mate. In this method, a complex mate (e.g. Hinge, Gear, Screw) is replaced by a certain number of simple mates (e.g. Coincidence, Parallel, Coaxial, Vertical) between simple elements (e.g. points, lines and planes). This method is more flexible but is also difficult to be apply in the dynamic analysis of complex assemblies.

(3) Replace the original mate with the "bushing" tool under the "Analysis" tab of the mate parameter settings. This method converts the rigid constraint of a certain mate on the DOF into a flexible constraint that can produce small deformation under a specific stiffness and damping coefficient. The small deformation value can then be used to calculate the force at the mate. In comparison to (2), this method is more convenient to apply, and the analysis of the actual force distribution is simpler.

To implement method (3), we selected the "Analysis" tab in the "Hinge Mate" parameter and selected the "Bushing" tool. Then, we set the stiffness value (Isotropic) according to the assumed deformation displacement (e.g. 1 mm and 1°), and continuously adjusted the damping value (Isotropic) according to the smoothness of the stress-time curve. The final adjusted "Bushing" parameters are shown in Table 3.

Table 3

Connection between parts

Mates	Bushing			
	Type	Stiffness	Damping	Force
Hinge (Left)	Translational	1200kN/mm	2kN • s/mm	0
	Rotational	500kN • m/°	5kN • m • s/°	0
Hinge (Right)	Translational	1200kN/mm	2kN • s/mm	0
	Rotational	500kN • m/°	5kN • m • s/°	0

2.5 Redundant constraints

According to the actual motion of the equipment and the relational literature [11], the swing arm can only reach the specified angular displacement after several cycles of repeated loading. The change of angular displacement can be described by

$$\theta = 120° \times \sin\left(t \times \frac{\pi}{120}\right) \times \cos\left(t \times \frac{40\pi}{120}\right) \tag{1}$$

where θ is the angular displacement of the swing arm (°) and t is the simulation time (s). The sine is used to control the amplitude of the swing arm, and the cosine can control the period of the swing arm as the second factor. In this paper, the whole process is simulated 120 seconds, as 20 cycles, and a cycle means the angular displacement from zero to a positive maximum to zero again and then from zero to a negative maximum to zero again. We set the simulation parameters according to the following steps:

(1) Move the time pointer to the beginning of the timeline.

(2) Add global gravity, with a direction of -y and acceleration = 9.8m/s^2.

(3) Add a "Motor" in the form of "Expression". The loading position is the cylinder at the upper end of the swing arm and the loading direction is clockwise. The angular displacement-time curve of the swing arm is shown in Fig. 3.

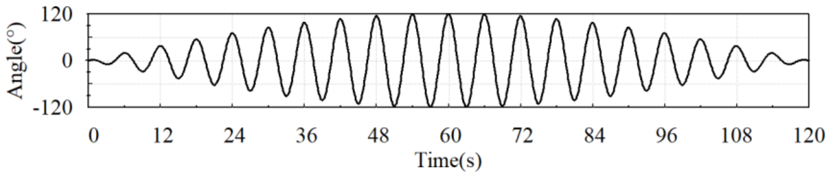

Fig. 3. The angular displacement-time curve

(4) Add another "Motor" in "Segments", with the loading position at the cylinder at the upper end of the rotary frisbee. Using the "component to move relative to" tool, select the swing arm, and set the rotary frisbee to accelerate linearly to 10 rpm by t = 3 seconds. The angular velocity-time curve of the rotary frisbee is shown in Fig. 4.

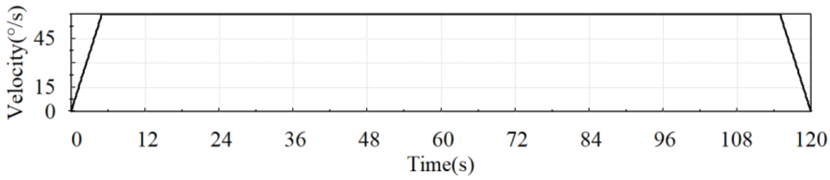

Fig. 4. The angular velocity-time curve of the rotary frisbee

(5) Add a datum surface coincidence constraint between the swing arm and the assembly to specify the initial position of the mechanism's motion. Then, compress the mate during motion analysis.

(6) Finally, set the simulation accuracy to 25 frames per second and other parameters as default.

3. Results extraction and analysis

3.1 Simulation results

After the simulation was complete, we selected the option of "Results and Plots", the category of "Forces", the subcategory of "Reaction Force" or "Reaction Moment", and extracted the results of the components from different directions. The analysis object was "Hinge + any surface of spindle", and the default reference frame was the global coordinate system. After extracting the results of "hinge" on both sides, it was found that the stress-time curves of each force component and the force magnitude were corresponding on each side. Accordingly, the unilateral extraction results are shown in Figures 5 and 6.

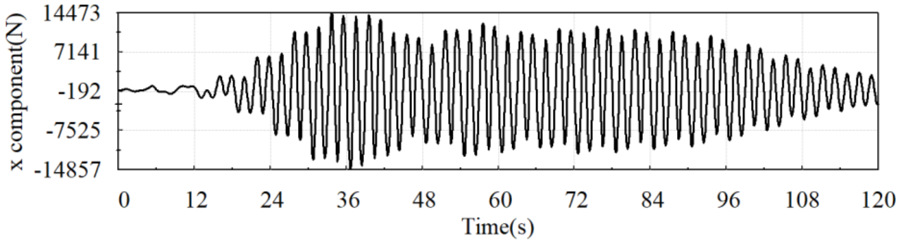

(a) *x* component reaction force - time curve

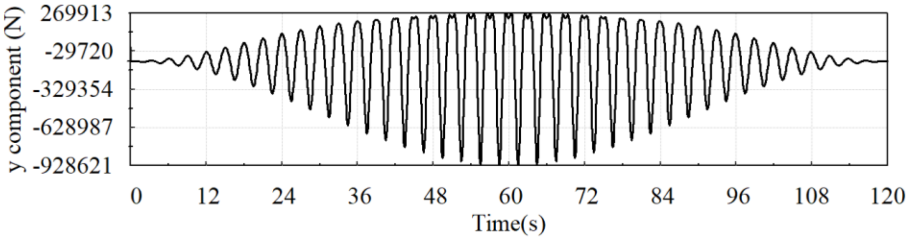

(b) *y* component reaction force - time curve

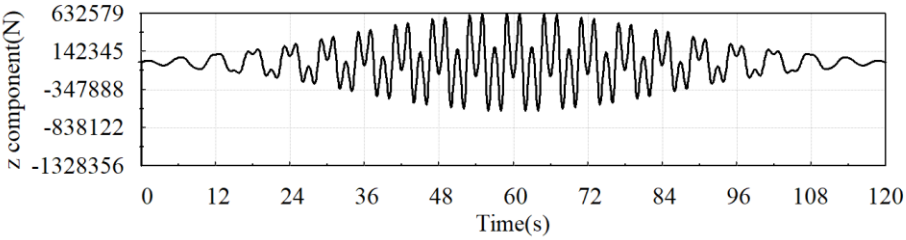

(c) *z* component reaction force - time curve

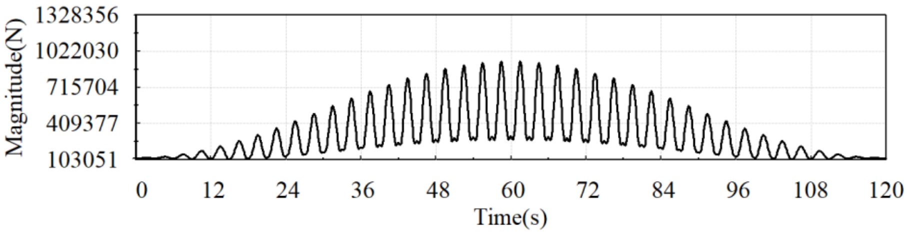

(d) Magnitude-time curve of reaction force

Fig. 5. Swing arm-spindle unilateral reaction force-time curves

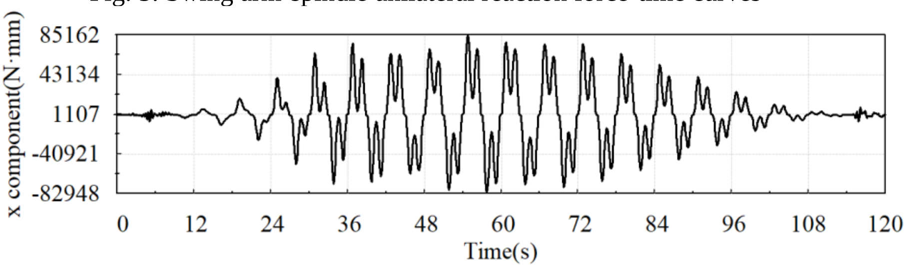

(a) *x* component reaction moment - time curve

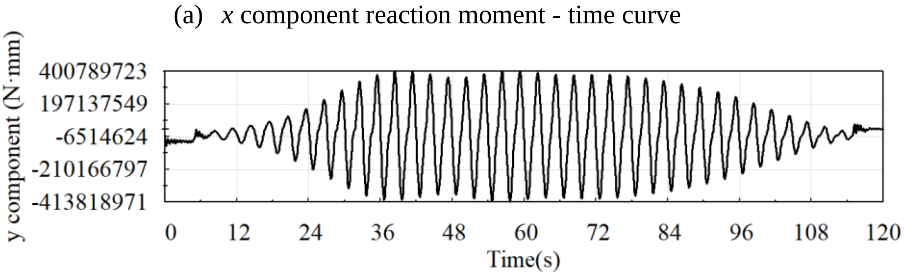

(b) *y* component reaction moment - time curve

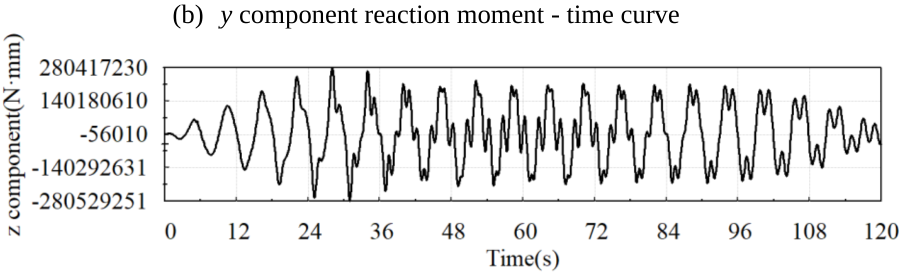

(c) *z* component reaction moment - time curve

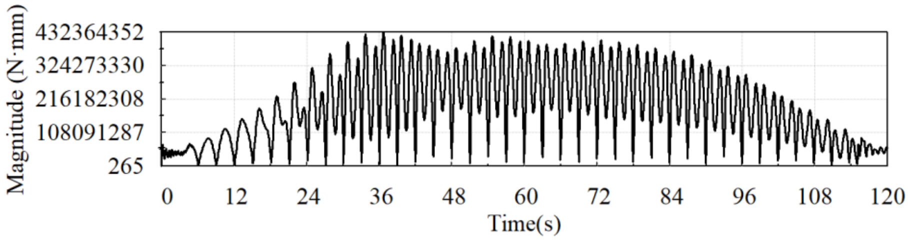

(d) Magnitude-time curve of reaction moment

Fig. 6. Swing arm-spindle unilateral reaction moment-time curves

From the reaction force-time curves, within a short period from the simulation start, the peak force was reached due to the initial motion of the swing arm under the force of gravity. The "bushing" tools need this period to establish the resistance velocity as this initial acceleration is a rapid change. Thus, the peak can be ignored in the analysis. To accurately analyze the dynamic characteristics of the mechanism within a short period after starting, the initial forces and torques of the "bushing" parameters can be set to “offset.”

3.2 Comparative analysis between simulation results and theoretical calculation

3.2.1 Theoretical calculation

In some researches [10,12], the equipment is simplified to a pendulum model. For the load on the spindle, only the centrifugal force was considered and the reaction moment of the gyroscopic effect was ignored. In this paper, we approximately calculated the reaction force and reaction moment values of the load on the spindle by rigid-body dynamical theories of fixed point motion.

The moment when the swing angle of the swing arm decreases from 120° to 0° for the first time (corresponding to t=61.5s in Figure 3) is selected for calculation. At this time, the axis of the swing arm is in the vertical position, and the centrifugal force reaches the maximum.

According to the rigid-body dynamics model, the distance between the gravity center of the swinging part and the axis of the spindle is *e* = 14.825m. The maximum linear velocity of the gravity center v_m can be written as

$$v_m = \sqrt{2gh} = \sqrt{2g(e + e \cdot \sin 30°)} = 20.88\mathrm{m/s} \tag{2}$$

where g is the acceleration of gravity (m/s^2) and h is the maximum height difference of the gravity center (m).

The maximum angular velocity of the gravity center ω_m can be written as

$$\omega_m = \frac{v_m}{e} = 1.408\mathrm{rad/s} \tag{3}$$

The centripetal acceleration of the gravity center a can be written as

$$a = e \cdot {\omega_m}^2 = 29.39\mathrm{m/s^2} \tag{4}$$

The overall centrifugal force of the swing part F_1 can be written as

$$F_1 = m_1(g + a) = 899.88\text{kN} \quad (5)$$

where m_1 is the mass of the swing part (kg).

According to the precession equation of the gyroscopic approximation theory, the reaction moment caused by the rotation $\overrightarrow{M_R}$ can be written as

$$\overrightarrow{M_R} = J_Z \overrightarrow{\omega_1} \times \overrightarrow{\omega_2} \quad (6)$$

where $\overrightarrow{M_R}$ is the gyroscopic reaction moment and its direction determined by the right hand rule is -*z* (kN · m); J_Z is the moment of inertia of the rotating part relative to its axis, and the value is 581972.65kg·m^2; $\overrightarrow{\omega_1}$ is the rotation angular velocity of the rotating part, the direction is +*y*, the value is 1.047rad/s; $\overrightarrow{\omega_2}$ is the angular precession velocity of the rotating part, the direction is +*x*, the value is 1.408rad/s.

The relevant data are substituted into equation (6) , and the result is $\overrightarrow{M_R} = 858.09\text{kN} \cdot \text{m}$. Moreover, the distance between the bilateral support center is 1.75m, and the reaction force of the spindle caused by the gyroscopic reaction moment F_2 can be written as

$$F_2 = \frac{M_R}{1.75} = \frac{858.09}{1.75} = 490.34\text{kN} \quad (7)$$

The force of the unilateral bearing F can be written as

$$F = \frac{(F_1 + 2 \cdot F_2)}{2} = 940.18\text{kN} \quad (8)$$

The reaction moment of the unilateral bearing caused by the gyroscope effect M can be written as

$$M = \frac{M_R}{2} = \frac{858.09}{2} = 429.05\text{kN} \cdot \text{m} \quad (9)$$

3.2.2 Contrastive Analysis

Compared the simulation results with the theoretical calculation, the maximum of each component and magnitude of force on the spindle are listed in Table 4.

Table 4

Simulation and theoretical calculation results

Analysis of the Position			Hinge Mate (Left)	Hinge Mate (Right)
Simulation Data	Maximum Reaction Force(kN)	Magnitude	929.88	929.88
		x component	14.86	14.86
		y component	929.62	928.62
		z component	632.58	632.58
	Maximum Reaction Moment(kN·m)	Magnitude	432.36	432.36
		x component	0.085	0.085
		y component	413.82	413.82
		z component	280.53	280.53

Theoretic Calculation (t=61.5s)	Maximum Reaction Force F (kN)	940.18
	Maximum Reaction Moment M (kN·m)	429.05

Based on a comprehensive analysis of the results, the following conclusions can be drawn:

(1) The two ends of "hinge" symmetrically share the reaction force transferred by the swing arm to the spindle, whose direction changes periodically with changes in the angle of swing motion. The maximum reaction force on the unilateral side of the spindle is 929.88kN, and the corresponding maximum reaction force is when the rotary frisbee reaches its lowest point. The reaction force is predominantly in the y-direction.

(2) On both ends of the "hinge", a symmetrical share of the swing arm is passed to the spindle, with a maximum reaction moment magnitude of 432.36kN·m. This is mainly concentrated in the y-direction component (corresponding to the horizontal reaction moment), demonstrating that the spindle force is affected by the gyroscopic effect and that cannot be ignored. Finally, this result indicates that there is a large deviation from the real-world case when the equipment is simplified to a pendulum model for theoretical calculation.

(3) The theoretical calculation shows that the maximum reaction force and the maximum reaction moment in the unilateral support are 940.18kN and 429.05kN·m respectively. Compared with the simulation results, we can obtain the maximum error of reaction force and reaction moment are 1.11% and 0.77% respectively. The simulation results are basically consistent with the theoretical calculation, which proves further the practicability and effectiveness of this simulation method. Moreover, the results also show that the gyroscopic effect has a great influence on spindle load and should be considered in the analysis and calculation.

4. Conclusion

(1) Based on the virtual prototype technology, the dynamic simulation analysis of the hanging spindle of the Giant Frisbee under the condition of full load is realized, and the theoretical dynamic calculation is carried out at the same time. The results show that the dynamic results can be obtained by setting the reasonable bushing parameters, and the method is more effective and reasonable.

(2) This method can provide a reference basis for solving the redundant constraints in virtual analysis, and can speed up the design speed and improve the design quality, which has a good engineering technology application prospect.

(3) This method has important reference significance for the in-depth study of dynamic characteristics of components with complex constraints by using virtual prototyping technology.

Acknowledgements

We would like to thank Editage (www.editage.cn) for English language editing.

REFERENCES

[1]. *R. Parpală*, "Virtual Design of a Machine Tool Feed Drive System", in Journal of UPB Scientific Bulletin, Series D: Mechanical Engineering, **vol. 71**, no. 4, 2009, pp. 131-140.
[2]. *I. Ghionea,* "Optimization Approach to Conception of a Mechanical Part Using CAD/FEM Techniques", in Journal of UPB Scientific Bulletin, Series D: Mechanical Engineering, **vol. 71**, no. 4, 2009, pp. 43-52.
[3]. *A. Bourebbou, M. Hacini, M. Assas, et al.*, "Toolpath Simulation of 3-axis Parallel Machine Tool Using Geometrical Model", in Journal of UPB Scientific Bulletin, Series D: Mechanical Engineering, **vol. 80**, no. 4, 2018, pp. 15-26.
[4]. *W. Marek,* "Joint Reaction Forces in Multibody Systems with Redundant Constraints", in Multibody System Dynamics, **vol. 14**, no. 01, Aug. 2005, pp. 23-46.
[5]. *W. Marek, F. Janusz,* "Solvability of Reactions in Rigid Multibody Systems with Redundant Nonholonomic Constraints", in Multibody System Dynamics, **vol. 30**, no. 02, Aug. 2013, pp. 153-171.
[6]. *H. Yu, J. Zhang, H. Wang,* "Dynamic Performance of Over-Constrained Planar Mechanisms with Multiple Revolute Clearance Joints", in Proceedings of the Institution of Mechanical Engineers, Part C: Journal of Mechanical Engineering Science, **vol. 232**, no. 19, Oct. 2018, pp. 3524-3537.
[7]. *Y. Wang, S. Yao, J. Liu, et al.,* "Fast Implementation of Virtual Prototyping Modeling Based on Assembly Model", in Journal of System Simulation, **vol. 28**, no. 09, Sept. 2016, pp. 1937-1944.
[8]. *D. Huang, X. Zou, X. Liao,* "Dynamic Simulation and Analysis Based on Pro/E of the Translational Platform with Redundant Constraints", in Journal of University of Electronic Science and Technology of China, **vol. 38**, no. 06, Nov. 2009, pp. 1042-1046.
[9]. *X. Liu,* Study on Practicable Simulation Software of Mechanical System Virtual Prototyping, Ph.D. Thesis, China Agricultural University, 2001.
[10]. *S. Yan,* Structure Analysis and Test Research on Big Pendulum of Amusement Equipment, M.A. Thesis, Taiyuan University of Technology, 2015.
[11]. *W. Lin,* The Risk Assessment and Prevention Research of Typical Amusement Rides at Complex Working Condition, Ph.D. Thesis, Beijing University of Chemical Technology, 2013.
[12]. *J. Zhao*, "Dynamics Analysis of Big Pendulum Based on ANSYS Workbench", in Mechanical Research and Application, **vol. 32**, no. 01, Feb. 2019, pp. 44-47.
[13]. *Y. Li, M. Han*, "Based on SolidWorks-Motion Large Rotary Amusement Equipment Dynamic Simulation Analysis", in Journal of Machinery Design and Manufacture, Mar. 2013, pp. 51-53.
[14]. *Y. Li, L. Wang, Y. Song, et al.,* "Rigid Body Dynamics Analysis in Design of Cantilever Beam of Entertainment Equipment Based on SolidWorks-Motion", in Proceedings of 2017 8th International Conference on Mechanical and Intelligent Manufacturing Technologies, ICMIMT 2017, May. 2017, pp. 69-73.
[15]. *C. Chen, Q. Hu,* SolidWorks-Motion Dynamic Simulation Tutorial, Beijing: China Machine Press, 2014.